J. Plasma Physics (2008), *vol.* 74, *part* 1, *pp.* 79–90. © 2007 Cambridge University Press
doi:10.1017/S0022377807006563 First published online 11 April 2007 Printed in the United Kingdom

On the effect of baryon loading in magnetized counterstreaming plasmas. I. Analytical investigation

R. C. TAUTZ[1] and J.-I. SAKAI[2]

[1] Institut für Theoretische Physik, Lehrstuhl IV: Weltraum-und Astrophysik, Ruhr-Universität Bochum, D-44780 Bochum, Germany

[2] Laboratory for Plasma Astrophysics, Faculty of Engineering, Toyama University, 3190, Gofuku, Toyama 930-8555, Japan

(Received 25 October 2006, revised 24 January 2007, accepted 12 February 2007)

Abstract. Assuming a non-relativistic three species electron–positron–ion plasma, the counterstreaming instability is investigated for waves propagating parallel and perpendicular to a homogeneous background magnetic field. From the exact linear dispersion relations, it is shown analytically how the growth rates change with increasing baryon loading, revealing new characteristics that cannot be found either for an unmagnetized plasma involving three particle species or for a plasma with only two particle species.

1. Introduction

The classic paper of Weibel (1959) showing the presence of kinetic instabilities in a homogeneous plasma with temperature anisotropy, where the instability depends solely on the bulk properties of the plasma and is independent of resonant wave–particle effects, has been the catalyst for a plethora of research. With astrophysical applications in mind, this interest is underscored by the observations of highly relativistic plasmas, highly energetic particles and their associated radiation (see, e.g., Schlickeiser (2003) for an introduction to the subject) and by the fact that the classic Weibel instability provides a mode growing exponentially in time but not propagating. The exponential growth of the linear phase eventually saturates (e.g. Kato (2005); see also Silva et al. (2003) for a discussion of the filamentation instability, which is related to the Weibel instability in that it also excites aperiodic fluctuations). In the following, the magnetic field grows further owing to coalescence processes of the current filaments that are created during the linear growth phase (see, e.g., Bogdan and Lerche 1985). The maximum magnetic field strength excited by the Weibel instability can be investigated by, for example, comparing the energy density of the magnetic field to the total energy density (Wiersma and Achterberg 2004). Doing so, it can be shown that for the case of, for example, gamma-ray bursts, the proton-driven Weibel instability is *not* a suitable candidate for the dissipation of the kinetic energy.

Detailed examination has been focused on counterstreaming plasma distributions, because, as first shown by Fried (1959), in such cases unstable Weibel modes

https://doi.org/10.1017/S0022377807006563 Published online by Cambridge University Press

are excited too. Since then, there has been a large amount of general work on this subject (e.g. Bornatici and Lee 1970; Lee and Armstrong 1971; Yoon and Davidson 1987; Haruki and Sakai 2003; Saito and Sakai 2004; Tzoufras et al. 2006; Tautz and Sakai 2006; Tautz and Schlickeiser 2005a, b, 2006a, b), where in most of these articles a background magnetic field has been assumed to be present in the direction of the counterstream. It has been found that many astrophysical scenarios can be described by means of counterstreaming plasma distributions, ranging from possible creation mechanisms of cosmological magnetic fields (e.g. Schlickeiser and Shukla 2003; Sakai et al. 2004; Schlickeiser 2005) through relativistic jets such as that from Active Galactic Nuclei and gamma-ray bursts (e.g. Dieckmann et al. (2006) and Tautz and Lerche (2006); see also Piran (2000), Mészáros (2002), and Piran (2004) for a detailed introduction to the physics of gamma-ray bursts) to local phenomena in the solar system (e.g. Miller and Viñas 1993; Canu et al. 1993; Bauer et al. 2001; Szego et al. 2003; Krupp et al. 2004; Crooker et al. 2004).

In the majority of situations, only the cases of either an electron–positron plasma (often leading to simplified equations) or an electron–proton (electron–ion) plasma have been considered. In a recent work (Fiore et al. 2006), however, the 'baryon loading' of an electron–positron plasma (i.e. the addition of a certain number of ions instead of electrons and positrons only) was investigated and it was shown that, although thermal effects are known to slow down the instability (Lee 1969), the baryon loading can sustain the instability even for high temperatures that would, normally, strongly suppress the instability. Inspired by this article, in the present paper we investigate the general effect of baryon loading on the dispersion relations of Weibel modes in counterstreaming Maxwellians that consist of electrons, protons and ions. Whereas in Fiore et al. (2006) an unmagnetized plasma was considered, in the current paper a homogeneous background magnetic field $\mathbf{B}_0$ is assumed to be present in the direction parallel to the counterstream. Because the inclusion of relativistic effects would add too many layers of technical difficulties to the problem (e.g. Lazar and Schlickeiser 2006; Tautz et al. 2007) even for a non-magnetized plasma (e.g. Tautz and Schlickeiser 2005a; Schaefer-Rolffs et al. 2006), the present investigation will be limited to non-relativistic thermal and streaming velocities. It is possible, at least in principle, to treat relativistic plasma instabilities including magnetic field effects by using a fluid approach (e.g. Bret et al. 2006). However, a kinetic treatment is far more complex and thus reveals new types of instabilities that are not derivable by any other procedure, as pointed out in Tautz et al. (2006a). Furthermore, it is known that a strong background magnetic field eventually suppresses the instability (e.g. Stockem et al. 2006; Tautz et al. 2007). Our values for the homogeneoues background magnetic field are, therefore, chosen well below this limit.

This paper is organized as follows: First, in Sec. 2, the distribution function and the basic parameters are introduced. In Secs 3 and 4, the dispersion relations (Tautz and Schlickeiser 2005a, b, 2006a, b) will be investigated analytically and the range of unstable wavenumbers will be calculated for the cases of parallel and perpendicular wave propagation with respect to the background magnetic field, respectively. From these results, the maximum growth rates and the associated maximum unstable wavenumber will be determined. The case of oblique wave propagation at arbitrary angles to the background magnetic field (cf., e.g., Bret et al. 2005) is not examined in the current work. Finally, Sec. 5 provides a short summary and discussion of the results obtained.

https://doi.org/10.1017/S0022377807006563 Published online by Cambridge University Press

2. Basic parameters

The distribution function for each particle species a is constructed of two Maxwellians that are counterstreaming parallel to a homogeneous background magnetic field $\mathbf{B}_0$ and have, in general, different temperatures (described by the temperature anisotropy parameter τ) in the directions parallel and perpendicular to $\mathbf{B}_0$, respectively:

$$f_a = (2\pi^{3/2} v_{\mathrm{th},a}^3 \tau)^{-1} e^{-(v_x^2+v_y^2)/(v_{\mathrm{th},a}^2\tau)} \times [e^{-(v_z-v_0)^2/v_{\mathrm{th},a}^2} + e^{-(v_z+v_0)^2/v_{\mathrm{th},a}^2}]. \tag{2.1}$$

Here, v_0 and v_{th} denote the counterstreaming and parallel thermal velocity, respectively, that both have to be non-relativistic, i.e. small compared to the speed of light. The distribution function from (2.1) is normalized so that $\int \mathrm{d}^3 v\, f_a(\mathbf{v}) = 1$.

In all dispersion relations, a summation over the particle species a is carried out that, according to the basic *ansatz*, extends to electrons, positrons and ions. Whereas the streaming velocity v_0 is equal for all particle species, several other parameters are different for the three particle species and are, therefore, denoted with the indices e for electrons, p for positrons and i for ions. These parameters are as follows: (i) the ion thermal velocity that scales with the mass ratio as $v_{\mathrm{th,i}} = v_{\mathrm{th,e}}\mu^{-1/2}$; (ii) the positron plasma frequency that scales with the density ratio as $\omega_{\mathrm{p,p}} = \omega_{\mathrm{p,e}}\xi^{1/2}$; (iii) the ion plasma plasma frequency that scales with the density ratio and the mass ratio as $\omega_{\mathrm{p,i}} = \omega_{\mathrm{p,e}}(\xi/\mu)^{1/2}$; and (iv) the ion cyclotron frequency that scales with the mass ratio as $\Omega_{\mathrm{i}} = -\Omega_{\mathrm{e}}/\mu$.

Furthermore, numerical values are assumed for the different parameters as

$$\begin{gathered} \Omega_{\mathrm{e}} = -\Omega_{\mathrm{p}} = -0.2828\omega_{\mathrm{p,e}}, \\ \xi \equiv n_{\mathrm{p}}/n_{\mathrm{e}} \in \{0, 0.2, 0.5, 0.8, 1\}, \\ \mu \equiv m_{\mathrm{i}}/m_{\mathrm{e}} = 64, \\ \tau \equiv T_\perp/T_\parallel = 1, \\ v_{\mathrm{th,e}} = v_{\mathrm{th,p}} = 0.1c, \\ v_0 = 0.3c. \end{gathered} \tag{2.2}$$

The value of 64 for the mass ratio was chosen so that the computer time for a self-consistent particle-in-cell (PIC) simulation, which will be presented in a future paper of this series, is kept moderate but, on the other hand, allows for a clear distinction between positrons and ions.

In any case, the electron number density is half the total particle number density, so that the positron and ion number densities add up to the other half.

With the constraint of investigating the wave progation only in the directions parallel and perpendicular to the background magnetic field $\mathbf{B}_0$, six wave modes are known (e.g. Davidson 1983): the electrostatic and the two electromagnetic wave modes that propagate in the parallel direction, the ordinary-wave mode, the Bernstein wave mode and the extra-ordinary electromagnetic wave mode, where the latter three propagate in the perpendicular direction. Only the electromagnetic wave modes and the ordinary-wave mode are subject to Weibel-type instabilties that excite aperiodic waves (i.e. purely growing waves with no propagating component). In the present work, therefore, only these wave modes will be discussed.

https://doi.org/10.1017/S0022377807006563 Published online by Cambridge University Press

To avoid confusion, it should be mentioned that the term 'Weibel instability' originally referred to parallel propagating aperiodic waves only. However, it has become convention to name any other types of aperiodic waves as 'Weibel-type' modes. As has been shown by Tautz and Schlickeiser (2006a) from the dispersion relation of the ordinary-wave mode, the counterstreaming instability indeed excites perpendicularly propagating aperiodic fluctuations whose electric field vector is aligned with the flow direction; thus, the ordinary-wave mode can also excite Weibel-type fluctuations.

In turn, analytical expressions for the dispersion relation will be investigated. Special attention will be turned to the effect of increasing baryon loading in the dispersion relations of the electromagnetic wave mode and the ordinary-wave mode, and their growth rates as well as their maximum unstable wavenumbers will be calculated for the parameters given above.

3. Parallel wave propagation

The non-relativistic dispersion relation for the two electromagnetic wave modes that propagate parallel to the counterstream direction and have transverse polarization has the form (see Tautz and Schlickeiser 2005a, b)

$$0 = 1 - \sum_a \frac{c^2 k_\parallel^2 + \omega_{\mathrm{p},a}^2}{\omega^2} \mp \sum_a \frac{\omega_{\mathrm{p},a}^2}{\omega^2} \frac{\Omega_a}{k_\parallel v_{\mathrm{th},a}} \times \left[\varepsilon Z\left(\frac{\omega - k_\parallel v_0 \pm \Omega_a}{k_\parallel v_{\mathrm{th},a}} \right) + (1-\varepsilon) Z\left(\frac{\omega + k_\parallel v_0 \pm \Omega_a}{k_\parallel v_{\mathrm{th},a}} \right) \right] - \frac{\tau}{2} \sum_a \frac{\omega_{\mathrm{p},a}^2}{\omega^2} \times \left[\varepsilon Z'\left(\frac{\omega - k_\parallel v_0 \pm \Omega_a}{k_\parallel v_{\mathrm{th},a}} \right) + (1-\varepsilon) Z'\left(\frac{\omega + k_\parallel v_0 \pm \Omega_a}{k_\parallel v_{\mathrm{th},a}} \right) \right], \tag{3.1}$$

where $Z'(f)$ denotes the first derivative with respect to its argument f of the plasma dispersion function $Z(f)$ of Fried and Conte (1961, see Appendix A). These wave modes have transverse circular polarization and are named 'right-handed' (upper signs) and 'left-handed' (lower signs). Furthermore, this form allows for different relative intensities as described by the factor $\varepsilon \in (0, 1)$.

Furthermore, care has to be taken of the fact that the cyclotron frequency Ω_a has opposite sign for positively and negatively charged particles.

First, in Fig. 1, the growth rates for an unmagnetized plasma ($\mathbf{B}_0 = 0$) with zero counterstreaming velocity ($v_0 = 0$) is shown, where the instability is driven solely by a temperature anisotropy of $\tau = 2$. The different cases have the following properties: (i) the case of electrons and ions only (we shall call this the 'ion case') has the lowest growth rate ($\Gamma/\omega_{\mathrm{p,e}} = 0.0139$); (ii) the case of electrons and positrons only (the 'positron case') has the highest growth rate ($\Gamma/\omega_{\mathrm{p,e}} = 0.0199$); and (iii) the intermediate cases for different density ratios between $\xi = 0.2$ and $\xi = 0.8$ interpolate the two limiting cases. The same is true for the maximum unstable wavenumber, which is lowest (highest) for the ion (positron) case.

The case of a non-vanishing counterstream in a magnetized plasma, where the parameters from (3) are used, is shown in Figs 2 and 3. Here, the temperatures are taken to be isotropic ($\tau = 1$) and the instability is, therefore, driven solely by the counterstream. Although again the maximum growth rate becomes larger if ξ is

https://doi.org/10.1017/S0022377807006563 Published online by Cambridge University Press

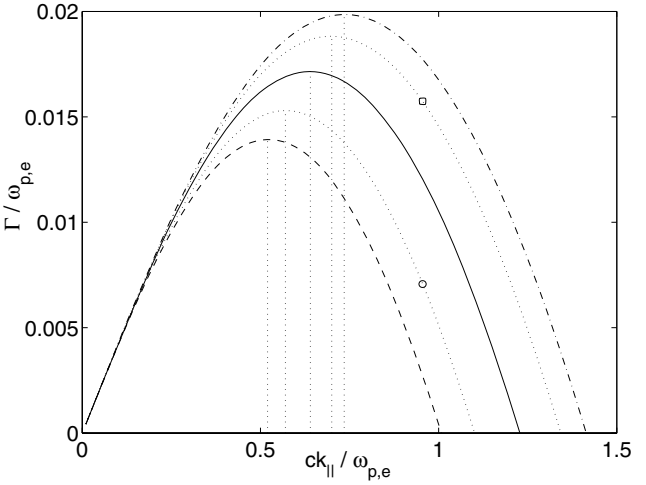


Figure 1. Growth rates of the electromagnetic mode for an unmagnetized plasma with anisotropic temperatures and zero counterstream velocity ($B_0 = 0$, $v_0 = 0$, $\tau = 2$). The following five cases are shown: (i) ions only (dashed line); (ii) 20% positrons (dotted line marked with a circle); (iii) half ions and half positrons (solid line); (iv) 20% ions (dotted line marked with a square); and (v) positrons only (dash-dotted line). Furthermore, the maximum growth rate and the associated wavenumber for each case is marked by a vertical dotted line.

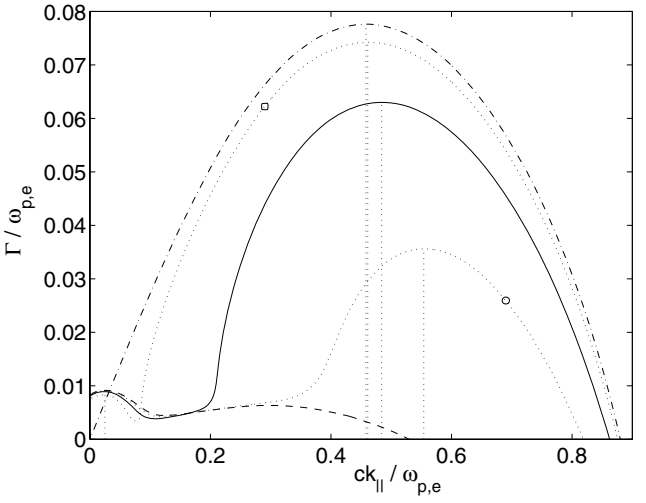


Figure 2. Growth rates of the electromagnetic mode for the parameters of (3). The following five cases are shown: (i) ions only (dashed line); (ii) 20% positrons (dotted line marked with a circle); (iii) half ions and half positrons (solid line); (iv) 20% ions (dotted line marked with a square); and (v) positrons only (dash–dotted line). Furthermore, the maximum growth rate and the associated wavenumber for each case is marked by a vertical dotted line.

varied from 0 to 1, the situation is, however, entirely different to the above case. Whereas the growth rate for the positron case has a single maximum, the growth rate for the ion case has two maxima, the first of which is also the global maximum. For the intermediate cases, there are always at least two maxima whenever ions

https://doi.org/10.1017/S0022377807006563 Published online by Cambridge University Press

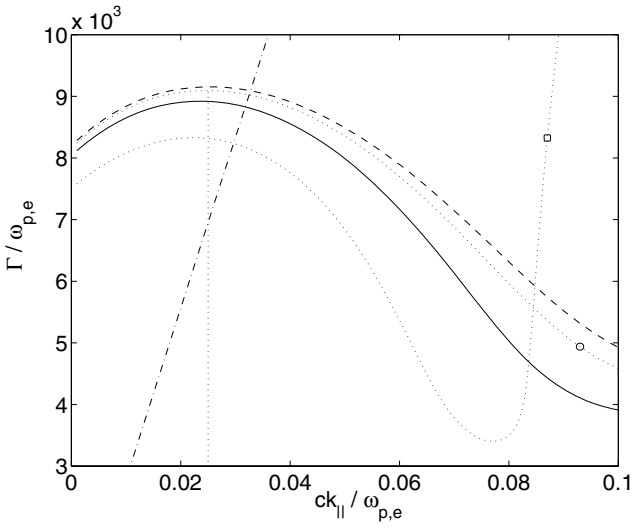


Figure 3. The range of small wavenumbers of Fig. 2, where all cases involving a fraction of protons have a second maximum in the growth rate. The vertical dotted line denotes the (global) maximum of the ion case.

are present. Which of the maxima is the global maximum depends on the value of ξ (see below).

This is an analogy to the fact that, in the presence of ions, Whistler waves are excited (e.g. Iwamoto 1993), which are absent in a leptonic plasma. However, as a referee has noted, Whistler waves are not aperiodic but have a non-vanishing real part of the wave frequency.

Furthermore, whereas the maximum unstable wavenumber of the first maximum is nearly constant, the position of the (global) maximum unstable wavenumber varies considerably and has its smallest (highest) value for the case of 80% positrons (100% ions). Note that, unlike in the previous case of an unmagnetized plasma or in the case of perpendicular wave propagation (see Sec. 4), it is *not* the positron case that yields the highest value for the maximum unstable wavenumber.

Note also that all curves in Figs 2 and 3 show the case of right-hand circularly polarized waves, corresponding to the upper signs in (3.1). The difference to the case of left-hand polarization is illustrated in Fig. 4 for $\xi = 0.05$ and is mainly important for small wavenumbers. The values for the maximum growth rate and the maximum unstable wavenumber differ significantly only for the first maximum. The second and third maxima remain nearly unchanged, indicating that the difference between left- and right-handed polarization becomes less important for an increasing fraction of positrons. Furthermore, Fig. 4 indicates that, when starting from an electron–ion plasma, the inclusion of a certain amount of positrons is *not* described by a simple transition between the ion and the positron cases; rather, completely new features are exhibited by the growth rate as a function of the wavenumber.

For completeness, the real part of the frequency for different values of the baryon loading is shown in Fig. 5. The curves shown there, however, correspond to a different solution of the dispersion relation than that shown in the figures before,

https://doi.org/10.1017/S0022377807006563 Published online by Cambridge University Press

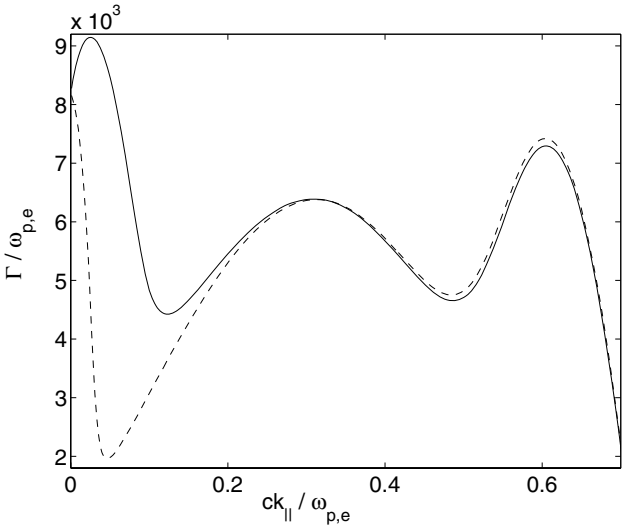


Figure 4. The difference between right-hand and left-hand polarization of the electromagnetic wave mode for $\xi = 0.05$, where now a third maximum can be seen. Note that, for the last maximum, the value for the maximum growth rate and the maximum unstable wavenumber remain nearly unchanged,whereas for the first maximum significant changes occur.

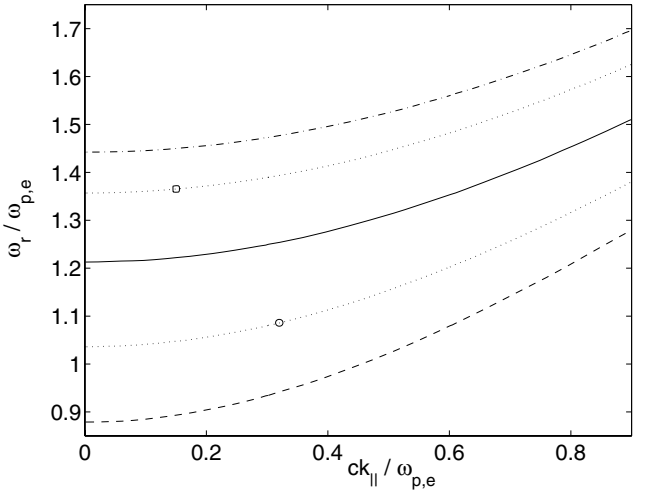


Figure 5. The real part of the frequency, $\omega_{\rm r}/\omega_{\rm p,e}$, for the electromagnetic wave mode. Shown are the cases of ions only (dashed line), 20% positrons (dotted line marked with a circle), half positrons and half ions (solid line), 80% positrons (dotted line marked with a square) and positrons only (dash–dot line).

because the solutions shown in Fig. 5 yield purely real frequencies with vanishing growth rates.

The other parallel propagating wave mode, namely the electrostatic mode, is unstable owing to the two-stream instability, which sets in when the flow speed exceeds the electron thermal speed by a factor of 1.3 (Bornatici and Lee 1970).

https://doi.org/10.1017/S0022377807006563 Published online by Cambridge University Press

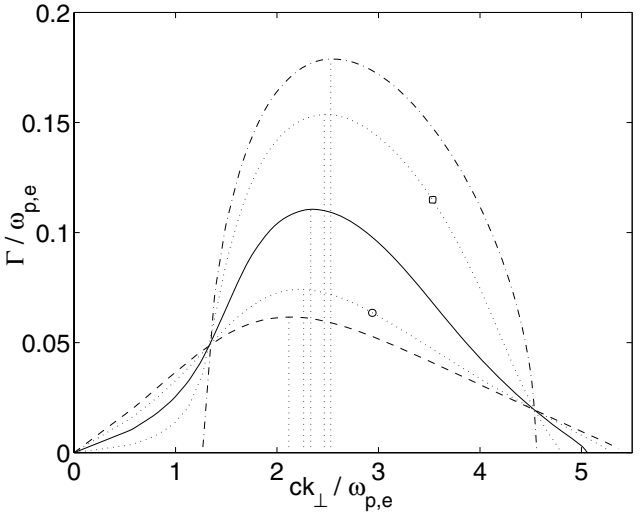


Figure 6. Growth rates of the ordinary-wave mode for the following five cases: (i) ions only (dashed line); (ii) 20% positrons (dotted line marked with a circle); (iii) half ions and half positrons (solid line); (iv) 20% ions(dotted line marked with a square); (v) positrons only (dash–dotted line). Again, the maximum growth rate and the associated wavenumber for each case is marked by a vertical dotted line. Note that all five lines intersect at two points.

The presence of mobile positrons will, certainly, modify this threshold, but in the limit of vanishing positron density the two-stream scenario is recovered (see also Spero and Sen 1968).

4. Perpendicular wave propagation

The dispersion relation for the ordinary-wave mode (see Tautz and Schlickeiser 2006a) can be expressed in terms of the hypergeometric function ${}_2F_2$ (see Appendix A) and reads

$$0 = 1 - \frac{c^2 k_\perp^2}{\omega^2} + \frac{1}{\tau}\sum_a \frac{\omega_{\mathrm{p},a}^2}{\omega^2}\left(1 + \tau + 2\frac{v_0^2}{v_{\mathrm{th},a}^2}\right) \times \left[1 - {}_2F_2\left(\frac{1}{2}, 1; 1 + \frac{\omega}{\Omega_a}, 1 - \frac{\omega}{\Omega_a}; -\left(\frac{k_\perp v_{\mathrm{th},a}}{\Omega_a}\right)^2\right)\right]. \tag{4.1}$$

The wave described by this dispersion relation has transverse polarization, with the electric field aligned with the direction of the background magnetic field. Furthermore, it should be noted that this wave mode is not affected by a different relative intensity of the two streams.

The growth rate of the ordinary-wave mode, corresponding to solutions of (4.1) with purely imaginary frequency, is shown in Fig. 6. For this wave mode the baryon loading merely results in an interpolation between the ion and positron cases (where the growth rate has its lowest value for the ion positron case and its highest value for the positron case). However, it should be noted that now for two wavenumber values all growth rates are equal as the range of unstable wavenumbers becomes narrower for an increasing amount of positrons.

https://doi.org/10.1017/S0022377807006563 Published online by Cambridge University Press

Table 1. Maximum growth rates and maximum unstable wavenumber for the electromagnetic wave mode (Index em) and for the ordinary-wave mode (Index ord).

$\xi = n_\mathrm{p}/n_\mathrm{e}$	$\Gamma_\mathrm{em}/\omega_\mathrm{p,e}$	$ck_\mathrm{em}/\omega_\mathrm{p,e}$	$\Gamma_\mathrm{ord}/\omega_\mathrm{p,e}$	$ck_\mathrm{ord}/\omega_\mathrm{p,e}$
0	0.0092	0.0250	0.0617	2.1166
0.2	0.0356	0.5540	0.0742	2.2627
0.5	0.0630	0.4840	0.1105	2.3324
0.8	0.0742	0.4610	0.1536	2.4658
1	0.0776	0.4580	0.1789	2.5298

Note also that the other perpendicular wave modes (the Bernstein wave mode and the extraordinary electromagnetic wave mode) are affected neither by the counterstream nor by a temperature anisotropy, as clearly shown in Tautz and Schlickeiser (2006a). Therefore, no unstable Weibel modes are excited from these dispersion relations.

5. Summary and discussion

In this series of papers, the effects of baryon loading in magnetized counterstreaming plasmas are investigated on the basis of non-relativistic linear dispersion relations and self-consistent PIC simulations. Therefore, a plasma with three particle species, namely electrons, positrons, and ions with a mass ratio of 64 was introduced. This first paper has investigated analytically the previously derived linear dispersion relations (Tautz and Schlickeiser 2005b, 2006a), and detailed examination has focused on the two cases of parallel and perpendicular wave propagation and the behavior of the respective growth rates and maximum unstable wavenumbers for increasing baryon loading (Table 1). In the case of counterstreaming plasmas, the (parallel propagating) electromagnetic wave mode and the (perpendicularly propagation) ordinary-wave mode are subject to aperiodic, i.e. purely growing, fluctuations excited by the Weibel instability.

In Sec. 3 it was shown that, in contrast to an unmagnetized plasma, the transition from a pure ion–electron plasma to a pure electron–positron plasma is not just a simple interpolation when a homogeneous background magnetic field is included. For parallel wave propagation, the electromagnetic wave mode has two branches, namely the right-handed and the left-handed circular polarized branches, that exhibit different growth rates especially at small wavenumbers and for a small fraction of positrons. In this case the wavenumber has three maxima, a feature that cannot be seen either for an electron–ion plasma (two maxima) or for an electron–positron plasma (one maximum) and arises, therefore, solely from the presence of three different particle species. The growth rate of the ordinary-wave mode, in contrast, shows a smooth transition between the two cases of an electron–ion plasma and an electron–positron plasma. However, at two discrete wavenumbers, all growth rates are equal because all graphs of the growth rates for different baryon loading values intersect at these two wavenumber values. The maximum unstable wavenumber simply shows a transition from higher to smaller values with increasing baryon loading. Furthermore, the range of unstable wavenumbers is narrowest for an electron–positron plasma and becomes increasingly broader for increasing baryon loading, eventually extending to $k = 0$ for an electron–ion plasma.

https://doi.org/10.1017/S0022377807006563 Published online by Cambridge University Press

Recently, the situation of a plasma with three particle species, two of which are positively charged, was investigated and it was shown that growing plasma fluctuations due to the Weibel instability are excited even for high temperatures. From the investigation presented here, where a homogeneous background magnetic was assumed, it can therefore be concluded that this situation gives rise to completely new features in the dispersion relations. These features cannot be seen either from the investigation of two particle species or from simple interpolation of the growth rate between the two cases of an electron–positron plasma and an electron–ion plasma and deserve, therefore, further investigation from theory as well as from observations.

Besides analytical theory, self-consistent PIC simulations are needed to confirm the results of this paper and to investigate the modification of oblique propagating wave modes due to the presence of three particle species. These simulations will be presented in a future paper of this series.

Acknowledgements

First, we would like to thank the two anonymous referees for very careful reading of the paper and helpful comments that improved the presentation of our results. This work was partially supported the Deutsche Forschungsgemeinschaft (DFG) through grant No. Schl201/17-1 and Sonderforschungsbereich 591. One of the authors (R. C. Tautz) thanks the Deutsche Physikalische Gesellschaft (DPG) and the DFG for offering the opportunity of a two months research stay in Japan.

Appendix A. Special functions

The plasma dispersion function (Z function, see Fried and Conte (1961)) and its first derivative with respect to the argument f can be written as

$$Z(f) = i\sqrt{\pi}\, e^{-f^2}[1 + \mathrm{erfi}(f)], \tag{A 1a}$$

$$Z'(f) = -2 - 2i\sqrt{\pi}\, e^{-f^2} f[1 + \mathrm{erfi}(f)], \tag{A 1b}$$

where $\mathrm{erfi}(f)$ denotes the imaginary error function, defined through

$$\mathrm{erfi}(f) = -i\,\mathrm{erf}(if) = \frac{2}{\sqrt{\pi}} \int_0^f dt\, e^{t^2}. \tag{A 2}$$

For numerical evaluation purposes of the dispersion relation, the improved two-pole approximation (Martín and González 1979) can be used, which is given by

$$Z(f) = \frac{b}{a - f} - \frac{b^*}{a^* + f}, \tag{A 3}$$

where the star denotes the complex conjugate and where

$$a = \frac{\sqrt{23\pi - 32 - 4\pi^2}}{2(4 - \pi)} - i\,\frac{\sqrt{\pi}}{2(4 - \pi)}, \tag{A 4a}$$

$$b = \frac{1}{2} + i\frac{2\pi - 5}{2}\sqrt{\frac{\pi}{23\pi - 32 - 4\pi^2}}. \tag{A 4b}$$

In Fig. A.1, the exact Z function and its first derivative are shown in comparison to the improved two-pole approximation. For small arguments, the agreement is

https://doi.org/10.1017/S0022377807006563 Published online by Cambridge University Press

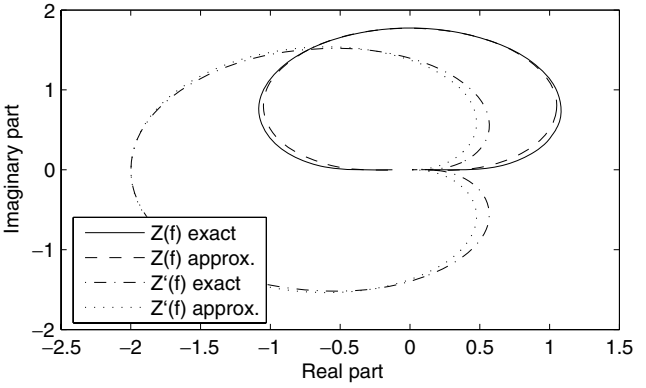


Figure A.1. A parametric plot of the plasma dispersion function $Z(f)$ and its first derivative $Z'(f)$ with respect to the argument f. Note that $Z(0) = i\sqrt{\pi}$ and $Z'(0) = -2$. The solid and dash-dotted lines show the exact Z function and its derivative, respectively, for real arguments. The dashed and dotted lines show the two-pole approximation of the Z function and its derivative, respectively.

very good; for large arguments, the agreement at least for $Z(f)$ is very good as well.

The hypergeometric function ${}_2F_2$ (see, e.g., Gradshteyn and Ryzhik 2000) is defined through the following infinite series:

$$ {}_2F_2\Big(a, b; c, d; z\Big) = \sum_{k=0}^{\infty} \frac{z^k}{k!} \frac{\Gamma(a+k)\Gamma(b+k)}{\Gamma(c+k)\Gamma(d+k)} \frac{\Gamma(c)\Gamma(d)}{\Gamma(a)\Gamma(b)}, \tag{A 5} $$

where $\Gamma(x)$ denotes the Gamma function.

References

Bauer, T. M., Treumann, R. A. and Baumjohann, W. 2001 *Ann. Geophys.* **19**, 1065.

Bogdan, T. J. and Lerche, I. 1985 *Astrophys. J.* **296**, 719.

Bornatici, M. and Lee, K. F. 1970 *Phys. Fluids* **13**, 3007.

Bret, A., Dieckmann, M. E. and Deutsch, C. 2006 *Phys. Plasmas* **13**, 082109.

Bret, A., Firpo, M. C. and Deutsch, C. 2005 *Phys. Rev. Lett.* **94**, 115002.

Canu, P., Cornilleau-Wehrlin, N., de Villedary, C., Kellogg, P. J., Harvey, C. C. and MacDowall, R. J. 1993 *Planet. Space Sci.* **41**, 811.

Crooker, N. U., Forsyth, R., Rees, A., Gosling, J. T. and Kahler, S. W. 2004 *J. Geophys. Res.* **109**, A06110.

Davidson, R. C. 1983 *Handbook of Plasma Physics*, Vol. 1 (ed. M. N. Rosenbluth and R. Z. Sagdeev). Amsterdam: North-Holland, p. 519.

Dieckmann, M. E., Shukla, P. K. and Drury, L. O. C. 2006 *Mon. Not. R. Astron. Soc.* **367**, 1072.

Fiore, M., Silva, L. O., Ren, C., Tzoufras, M. A. and Mori, W. B. 2006 *Mon. Not. R. Astron. Soc.* **372**, 1851.

Fried, B. D. 1959 *Phys. Fluids* **2**, 337.

Fried, B. D. and Conte, S. D. 1961 *The Plasma Dispersion Function*. New York: Academic Press.

Gradshteyn, I. S. and Ryzhik, I. N. 2000 *Table of Integrals, Series, and Products*. New York: Academic Press.

https://doi.org/10.1017/S0022377807006563 Published online by Cambridge University Press

Haruki, T. and Sakai, J.-I. 2003 *Phys. Plasmas* **10**, 392.

Iwamoto, N. 1993 *Phys. Rev.* E **47**, 604.

Kato, T. N. 2005 *Phys. Plasmas* **12**, 080705

Krupp, N., Woch, J., Lagg, A., Livi, S., Mitchell, D. G., Krimigis, S. M., Dougherty, M. K., Hanlon, P. G., Armstrong, T. P. and Espinosa, S. A. 2004 *J. Geophys. Res.* **109**, A09S10.

Lapuerta, V. and Ahedo, E. 2002 *Phys. Plasmas* **9**, 1513.

Lazar, M. and Schlickeiser, R. 2006 *Phys. Plasmas* **13**, 012110.

Lee, K. F. 1969 *Phys. Rev.* **181**, 453.

Lee, K. F. and Armstrong, J. C. 1971 *Phys. Rev.* A **4**, 2087.

Martín, P. and González, M. A. 1979 *Phys. Fluids* **22**, 1413.

Mészáros, P. 2002 *Ann. Rev. Astron. Astrophys.* **40**, 137.

Miller, J. A. and Viñas, A. F. 1993 *Astrophys. J.* **412**, 386.

Piran, T. 2000 *Phys. Rep.* **333**, 529.

Piran, T. 2004 *Rev. Mod. Phys.* **76**, 1143.

Saito, S. and Sakai, J.-I. 2004 *Astrophys. J.* **602**, L41.

Sakai, J.-I., Schlickeiser, R. and Shukla, P. K. 2004 *Phys. Lett.* A **330**, 384.

Schaefer-Rolffs, U., Lerche, I. and Schlickeiser, R. 2006 *Phys. Plasmas* **13**, 012107.

Schlickeiser, R. 2003 *Cosmic Ray Astrophysics*. Berlin: Springer.

Schlickeiser, R. 2005 *Plasma Phys. Control. Fusion* **47**, A205.

Schlickeiser, R. and Shukla, P. K. 2003 *Astrophys. J.* **599**, L57.

Silva, L. O., Fonseca, R. A., Tonge, J. W., Dawson, J. M., Mori, W. B. and Medvedev, M. V. 2003 *Astrophys. J.* **596**, L121.

Spero, D. M. and Sen, A. K. 1968 *Phys. Fluids* **11**, 1524.

Stockem, A., Lerche, I. and Schlickeiser, R. 2006 *Astrophys. J.* **651**, 584.

Szego, K. et al. 2003 *J. Geophys. Res.* **108**, 1287.

Tautz, R. C. and Lerche, I.2006 *Astrophys. J.* **653**, 447.

Tautz, R. C., Lerche, I. and Schlickeiser, R. 2007 Non-resonant kinetic instabilities of a relativistic plasma in a uniform magnetic field: longitudinal and transverse mode coupling effects. *J. Math. Phys.* **48**, 013302.

Tautz, R. C. and Sakai, J.-I. 2006 *Phys. Plasmas* **14**, 012104.

Tautz, R. C. and Schlickeiser, R. 2005a *Phys. Plasmas* **12**, 072101.

Tautz, R. C. and Schlickeiser, R. 2005b *Phys. Plasmas* **12**, 122901.

Tautz, R. C. and Schlickeiser, R. 2006a *Phys. Plasmas* **13**, 062901.

Tautz, R. C. and Schlickeiser, R. 2006b *Phys. Plasmas* **13**, 109902 (erratum to Tautz and Schlickeiser 2006a).

Tzoufras, M., Ren, C., Tsung, F. S., Tonge, J. W., Mori, W. B., Fiore, M., Fonseca, R. A. and Silva, L. O. 2006 *Phys. Rev. Lett.* **96**, 105002.

Weibel, E. S. 1959 *Phys. Rev. Lett.* **2**, 83.

Wiersma, J. and Achterberg, A. 2004 *Astron. Astrophys.* **428**, 365.

Yoon, P. H. and Davidson, R. C. 1987 *Phys. Rev.* A **35**, 2718.

https://doi.org/10.1017/S0022377807006563 Published online by Cambridge University Press